MOLECULAR AND CELLULAR BIOLOGY, Jan. 2009, p. 471–482 Vol. 29, No. 2
0270-7306/09/$08.00+0 doi:10.1128/MCB.01352-08

Functional Dissection of Human and Mouse POT1 Proteins[▽]†

Wilhelm Palm,‡ Dirk Hockemeyer,§ Tatsuya Kibe, and Titia de Lange*

Laboratory for Cell Biology and Genetics, The Rockefeller University, New York, New York 10065

Received 25 August 2008/Returned for modification 8 October 2008/Accepted 20 October 2008

The single-stranded telomeric DNA binding protein POT1 protects mammalian chromosome ends from the ATR-dependent DNA damage response, regulates telomerase-mediated telomere extension, and limits 5′-end resection at telomere termini. Whereas most mammals have a single POT1 gene, mice have two POT1 proteins that are functionally distinct. POT1a represses the DNA damage response, and POT1b controls 5′-end resection. In contrast, as we report here, POT1a and POT1b do not differ in their ability to repress telomere recombination. By swapping domains, we show that the DNA binding domain of POT1a specifies its ability to repress the DNA damage response. However, no differences were detected in the in vitro DNA binding features of POT1a and POT1b. In contrast to the repression of ATR signaling by POT1a, the ability of POT1b to control 5′-end resection was found to require two regions in the C terminus, one corresponding to the TPP1 binding domain and a second representing a new domain located between amino acids (aa) 300 and 350. Interestingly, the DNA binding domain of human POT1 can replace that of POT1a to repress ATR signaling, and the POT1b region from aa 300 to 350 required for the regulation of the telomere terminus is functionally conserved in human POT1. Thus, human POT1 combines the features of POT1a and POT1b.

Mammalian chromosome ends associate with shelterin, the protein complex dedicated to telomere protection and homeostasis (reviewed in references 5 and 20). The DNA of mammalian telomeres consists of long arrays of double-stranded (ds) TTAGGG repeats ending in a single-stranded (ss) protrusion of the 3′ end, referred to as the 3′ overhang. The 3′-overhang strand can invade the duplex part of telomeres, forming a lariat structure called the t-loop (8). Three shelterin components interact with telomeric DNA. POT1 recognizes ss TTAGGG repeats and therefore can associate with the telomeric 3′ overhang as well as with the displaced strand at the base of the t-loop. TRF1 and TRF2 cover the duplex part of telomeric DNA, and they recruit the other shelterin components Rap1, TIN2, and TPP1 to telomeres through protein-protein interactions. POT1 cannot localize to telomeres alone but instead requires heterodimerization with TPP1; this interaction is crucial for the association of POT1 with telomeres, as TPP1 tethers POT1 to TRF1 and TRF2 by a TPP1-TIN2 bridge and improves the DNA binding affinity of POT1 (12, 19, 26).

Shelterin masks telomeres from the cellular machinery that recognizes and repairs DNA lesions. If shelterin function is perturbed, DNA damage response factors accumulate at telomeres, leading to the activation of the ATM and ATR kinase signaling pathways (2, 10, 15, 29). Distinct components of shelterin independently repress ATM and ATR signaling: TRF2 is required to prevent ATM activation at telomeres, while POT1 represses the activation of ATR (16). Dysfunctional telomeres trigger various DNA repair reactions and can be processed like dsDNA breaks through nonhomologous end joining or through homology-directed repair (HDR) (3, 24, 27, 29).

The ss telomeric DNA binding proteins are key players in telomere protection and telomere length regulation. POT1 is highly conserved in fission yeast, plants, *Caenorhabditis elegans*, and vertebrates, and it is homologous to TEBPα, the 3′-overhang binding protein of ciliates (1, 4, 7, 21, 23, 28). Most vertebrates, including humans, possess a single POT1 gene. In contrast, a recent duplication of POT1 within the rodent lineage gave rise to two POT1 orthologs, referred to as POT1a and POT1b. The knockout of mouse POT1a and POT1b has revealed remarkable functional divergence despite their recent emergence (10). POT1a is required to repress ATR activation at telomeres; POT1b is dispensable in this regard but can partially complement the loss of POT1a. On the other hand, POT1b regulates the nucleolytic processing of the 5′ end, which is involved in 3′-overhang genesis. POT1b deficiency results in the excessive resection of the 5′ end, leading to an increase of the 3′-overhang sequences as well as progressive telomere shortening (10, 11). Like POT1a, human POT1 is required to hide telomeres from DNA damage surveillance, and it can complement the loss of POT1a at mouse telomeres if coexpressed with human TPP1 (hTPP1) (10, 13, 16, 25). It has been speculated that POT1b harbors functions not conserved in its human homologue, as human POT1 does not complement POT1b in terms of the 3′-overhang regulation of mouse telomeres. However, human POT1 defines the 5′ end of human telomeres, which usually has the sequence ATC-5′, presumably by either regulating the nuclease that trims the 5′ end or protecting the sequence ATC-5′ from nucleolytic degradation (13, 22). Human POT1, therefore, may combine hallmarks of both POT1a and POT1b function, the repression of ATR, and the regulation of the nucleolytic processing of telomeres.

* Corresponding author. Mailing address: Laboratory for Cell Biology and Genetics, The Rockefeller University, 1230 York Avenue, New York, NY 10065-6399. Phone: (212) 327-8146. Fax: (212) 327-7147. E-mail: delange@mail.rockefeller.edu.

† Supplemental material for this article may be found at http://mcb.asm.org/.

‡ Present address: Max Planck Institute of Molecular Cell Biology and Genetics, Pfotenhauerstrasse 108, 01307 Dresden, Germany.

§ Present address: Whitehead Institute for Biomedical Research, 9 Cambridge Center, Boston, MA 02142.

▽ Published ahead of print on 27 October 2008.

The molecular basis for the functional differences between POT1a, POT1b, and human POT1 is not understood, and their high degree of sequence conservation impedes predictions from sequence comparison. Two distinct functional regions of POT1 are currently recognized, and both are crucial for its function: an N-terminal DNA binding domain comprising two oligonucleotide/oligosaccharide-binding (OB) folds and a C-terminal domain that mediates the interaction with TPP1 (12, 14, 17, 19, 30). However, no functional differences between POT1a and POT1b have been identified in these domains so far. The amino acid residues in the DNA binding domain of human POT1 that mediate its interaction with DNA are conserved in POT1a and POT1b, and N-terminal fragments of POT1a and POT1b were found to have similar DNA binding properties in vitro (9, 17). Similarly, the TPP1 interaction domain is conserved between POT1a and POT1b, and both associate with mouse TPP1 with equal efficiency. While cross-species interactions between human and mouse POT1 and TPP1 are poorly conserved, human POT1 can be efficiently recruited to mouse telomeres by the coexpression of hTPP1, arguing for the functional equivalence of the C termini of human and mouse POT1 proteins (12).

We set out to dissect the functional differences between POT1a and POT1b. We demonstrate their equivalence in yet another aspect of telomere protection, the repression of homologous recombination, and show that they possess similar DNA binding preferences. Using a set of chimeras of the human and mouse POT1 proteins, we assess the individual contributions of the N- and C-terminal parts of POT1 to its function. We show that the DNA binding domains of POT1a or hPOT, but not POT1b, fused to any TPP1 interaction domain, can efficiently repress ATR activation at telomeres. In contrast, a novel function residing in the POT1b C terminus is required for the control of nucleolytic 5′-end resection, and this property is partially conserved in human POT1.

MATERIALS AND METHODS

Cell lines and chimeric POT1 alleles. The POT1a$^{S/F}$, POT1b$^{S/F}$, and POT1a/b double knockout (DKO) (POT1a$^{S/F}$ POT1b$^{S/F}$) mouse embryo fibroblasts (MEFs) were described previously (10). POT1a$^{S/F}$ POT1b$^{S/+}$ Ku70$^{-/-}$, POT1a$^{F/+}$ POT1b$^{S/F}$ Ku70$^{-/-}$, and POT1a$^{S/F}$ POT1b$^{S/F}$ Ku70$^{-/-}$ MEFs were derived by standard mouse crosses. All MEFs were immortalized with SV40-large T. The Cre-mediated conditional deletion of POTa, POT1b, and TRF2 in wild-type or Ku70$^{-/-}$ MEFs that were immortalized with simian virus 40 large T antigen (SV40-large T) was performed through infection with retroviral Hit&Run Cre or adenoviral Cre (adenovirus 5-cytomegalovirus-Cre) as described previously (3, 10). The cloning strategy of the POT1 alleles is described in Fig. S2 in the supplemental material. All alleles were cloned into pWzl-N-myc, providing an N-terminal myc tag, and introduced by retroviral infection as described previously (12). Flag-tagged hTPP1 (12) was expressed from the pLPC-N-flag retroviral vector.

CO-FISH. The occurrence of telomere-sister chromatid exchanges (T-SCEs) at dysfunctional telomeres was monitored by chromosome orientation fluorescent in situ hybridization (CO-FISH) on mitotic cells collected 90 to 94 h after the deletion of POT1a, POT1b, or TRF2 with adenovirus 5-cytomegalovirus-Cre as described previously (3). The fluorescent probes used were 6-carboxytetramethylrhodamine–TelG (5′-[TTAGGG]$_3$-3′) and fluorescein isothiocyanate-TelC (5′-[CCCTAA]$_3$-3′). The principles of CO-FISH are schematized in Fig. 3 of reference 3.

Baculovirus-derived POT1a and POT1b and DNA binding assays. Full-length POT1a and POT1b were cloned as a BamHI-XhoI fragment into pFastBacHTb (Invitrogen), adding a His$_6$ tag to the N terminus. The generation of viral stocks and protein purification from 0.5 to 1.0 liter infected cells (48 h postinfection with a multiplicity of infection of 5) were performed following the manufacturer's recommendation. After purification, the protein was dialyzed against 20 mM HEPES (pH 7.9), 500 mM KCl, and 20% glycerol and stored in aliquots at −80°C. The protein concentration was determined by comparison to bovine serum albumin standards on Coomassie-stained gels.

All oligonucleotides were obtained from Sigma. Probes a, a3, and a5 were modeled on substrates described by Lei et al. (18) with an additional sequence change in a3 blocking the 5′ POT1 recognition site. For ss probes, oligonucleotides were labeled at the 5′ end with T4 polynucleotide kinase (New England Biolabs) and [γ-^{32}P]ATP and purified through a G25 column. For dsDNA, oligonucleotides were annealed, purified by polyacrylamide gel electrophoresis, labeled with Klenow enzyme (Roche) and [α-^{32}P]dCTP, and purified through a G25 column. The labeled oligonucleotides were extracted with phenol-chloroform-isoamyl alcohol, precipitated with 0.2 M sodium acetate (pH 5.5) and 2 volumes of ethyl alcohol at −80°C, and dissolved in 10 mM Tris (pH 8.0).

Binding reactions were performed in 10 μl of the following buffer: 50 mM Tris-HCl (pH 8.0), 0.1 mM dithiothreitol, 0.5% glycerol, 25 ng β-casein, 0.2 μg sonicated and denatured *Escherichia coli* DNA (mean size, 400 nucleotides [nt]), and probes at a final concentration of 0.5 nM. The protein was added last, and the mixture was incubated for 30 min at room temperature. A range of 0.156 to 40 nM of protein was used. Electrophoresis was performed with 0.8% agarose gels run in 0.2× Tris-borate–EDTA. The gels were run for 55 min at 140 V, fixed in 20% methanol–10% acetic acid, dried on Whatman DE81 paper at 80°C, and exposed on phosphorimaging screens.

Immunoblotting and immunofluorescence. Immunoblotting and immunofluorescence were performed as described previously (12). The myc epitope tag of retrovirally transduced POT1 variants was detected using mouse anti-myc 9E10 (Sigma); retrovirally transduced Flag-tagged hTPP1 was detected using either rabbit anti-hTPP1 (1151) or mouse anti-Flag M2 (Sigma). Immunofluorescence (IF) against TRF1 was performed using rabbit anti-mouse TRF1 (644). Telomere dysfunction-induced foci (TIFs) were monitored using mouse anti-γH2AX (Upstate Biotechnology, Lake Placid, NY) and rabbit anti-53BP1 (Novus).

Telomeric overhang assay. Telomeric overhangs were analyzed as described previously (2) (see Fig. S6 in the supplemental material for a schematic of the method). Overhang signals were measured 5 to 6 days after the deletion of POT1 genes through infection with Hit&Run Cre.

RESULTS

Repression of telomere recombination by POT1a and POT1b. Given their previously noted functional differences, we considered the possibility that POT1a and POT1b might also be distinct in their ability to repress HDR, another process presumed to involve the ssDNA at telomeres. HDR at telomeres can be detected by measuring T-SCEs. The Cre-mediated deletion of POT1a and POT1b from POT1a/b DKO MEFs did not result in a significant increase in the frequency of T-SCEs (Fig. 1B) ($P = 0.184$; six experiments; $n = 1{,}000$ chromosome ends/experiment). The individual deletion of POT1a or POT1b also did not induce T-SCEs (data not shown). We previously showed that T-SCEs at telomeres are repressed by two parallel pathways, one involving Ku70 and the second involving TRF2 (3). We therefore tested whether T-SCEs were similarly repressed by both the Ku70 and POT1 proteins. Accordingly, we generated POT1a$^{S/F}$ POT1b$^{S/F}$ Ku70$^{-/-}$ cells and tested their frequency of T-SCEs before and after the deletion of POT1a and -b. In the Ku70$^{-/-}$ setting, the deletion of POT1a and -b resulted in a high rate of T-SCEs, comparble to the phenotype of TRF2 deletion from Ku70 null cells (Fig. 1A, B, and C). To determine the relative contributions of POT1a and POT1b to the repression of T-SCEs in Ku70$^{-/-}$ cells, we generated Ku70$^{-/-}$ MEFs from which either POT1a or POT1b could be deleted. The deletion of either POT1a or POT1b did not induce T-SCEs in Ku70$^{-/-}$ cells, whereas the deletion of both proteins from cells processed in parallel again showed a high incidence of T-SCEs (Fig. 1C). These results indicate that both POT1a and POT1b have the

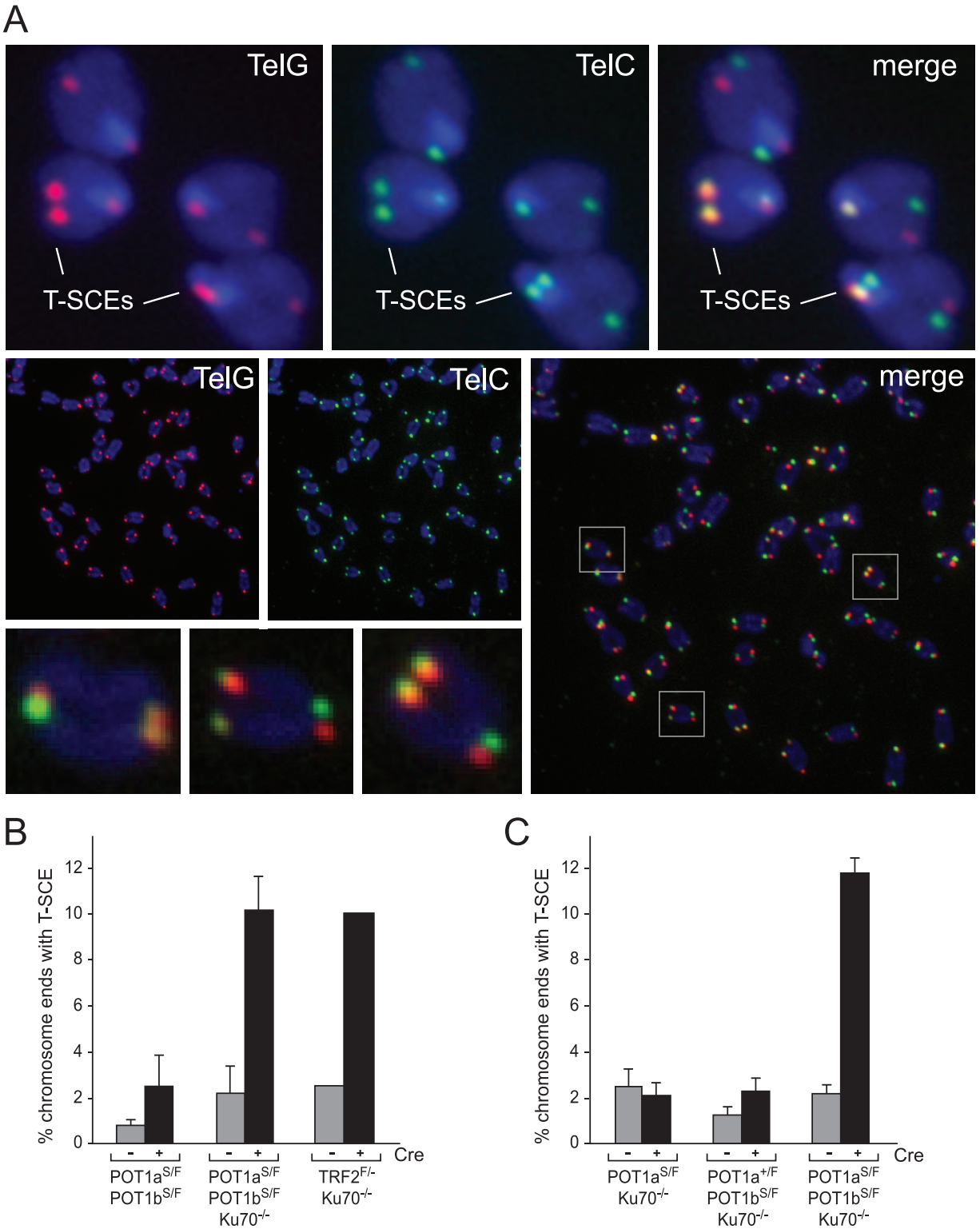

FIG. 1. POT1a and -b repress HDR in parallel with Ku70. (A) Examples of T-SCE events in POT1 DKO cells deficient for Ku70. CO-FISH analysis of POT1a$^{S/F}$ POT1b$^{S/F}$ Ku70$^{-/-}$ MEFs was performed 92 h after treatment with adenoviral Cre. Fluorescence signals of the TelG and TelC probes are depicted separately and merged. The enlargements depict chromosomes exhibiting T-SCEs. (B) Comparable induction of T-SCEs upon the simultaneous removal of POT1a and POT1b or the removal of TRF2 in Ku70$^{-/-}$ cells (POT1 DKO Ku70$^{-/-}$, $P = 0.006$ by Student's t test). Shown is the quantification of three independent CO-FISH experiments; at least 6,000 chromosome ends were analyzed for the POT1a$^{S/F}$ POT1b$^{S/F}$ cell lines and at least 4,000 for the TRF2$^{FLOX/-}$ Ku70$^{-/-}$ cell lines. The increase in T-SCE frequency after POT1a/b deletion in Ku70-proficient cells is not statistically significant ($P = 0.184$). (C) Both POT1a and POT1b alone are capable of suppressing T-SCEs in Ku70$^{-/-}$ MEFs. Shown is the quantification of three independent CO-FISH experiments. At least 1,000 chromosome ends were analyzed for each cell line in each experiment. Error bars in panels B and C indicate standard deviations.

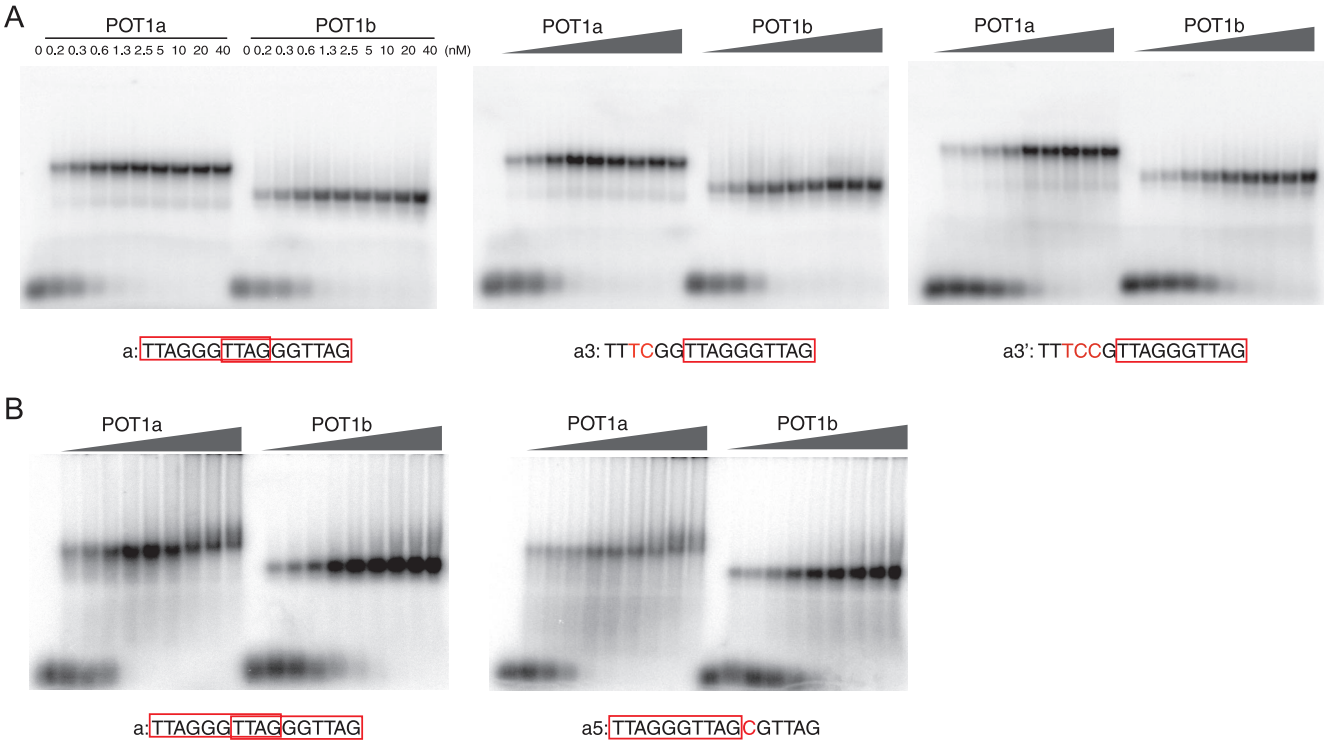

C

	a	a3	a3'	a5
POT1a	1.0 ±1.2	0.3 ±0.2	1.2 ±0.1	5.3, 2.3
POT1b	1.3 ±1.5	0.5 ±0.05	1.2 ±0.2	4.9, 13.7

FIG. 2. Binding of POT1a and -b to 3′ and 5′ telomeric sites. (A and B) Gel-shift reactions with the probes indicated below the gels and increasing amounts of POT1a and POT1b. (A) Binding of POT1a and -b to the probes a, a3, and a3′. The red letters indicate nucleotide changes that interfere with POT1 binding to the 5′ site. The minimal binding sites are highlighted by the red boxes. Protein amounts in each binding reaction are indicated above the lanes in the left panel, and the same amounts were used in other panels. (B) POT1a and -b bind to the telomeric site at a 5′ end with diminished affinity. The mutations in primer a5 block POT1a and POT1b from binding to the 3′ end of the probe. Probes with no POT1 recognition site are not bound by POT1a or -b. The gel shifts shown are representatives of three independent experiments. (C) Summary of the K_d values (nM) of POT1a and POT1b in gel-shift experiments with the indicated probes. Values derived from three or more experiments are given as averages with standard deviations. Where probes were tested only twice, both values are given. All experiments were done with POT1a and -b in parallel, and K_d values were derived from quantitative analysis of the phosphorimager data as shown in panels A and B.

ability to repress T-SCEs and that telomere-telomere recombination is unleashed only in Ku70-deficient cells that also lack either TRF2 or both POT1 proteins.

DNA binding features of POT1a and POT1b. Previous biochemical analysis of the DNA binding features of POT1a and POT1b showed that both proteins were proficient in binding to ssDNA substrates with the 12-nt sequence GGTTAGGG TTAG at the 3′ end (9). Because these studies were largely limited to 12- or 10-nt substrates and used truncated POT1 proteins representing the N-terminal DNA binding domains, we extended the analysis to full-length proteins and tested additional substrates. Full-length, N-terminally His_6-tagged mouse POT1a and POT1b were isolated from baculovirus-infected insect cells and used in gel-shift experiments. Both proteins bound telomeric substrates with approximately equal affinity (K_d of ~0.5 nM). In particular, the substrate with two overlapping sites and the substrate with one site at the 3′ end were equally bound by POT1a and POT1b, while a probe with the site at the 5′ end was a poor substrate for both proteins (Fig. 2 and data not shown).

As POT1b, but not POT1a, has the ability to protect the 5′ end from resection, we tested the interaction of the POT1 proteins with probes containing an ss-ds junction. The probes carried a short 3′ overhang with a single, nonterminal POT1 site. A control probe lacking a POT1 site in the 3′ overhang was not bound by POT1a or -b (data not shown). The 5′ end of the duplex part of the probes was either the ATC-5′ ending found at human telomeres or other endings in the C-strand sequence (Fig. 3; see also Fig. S1 in the supplemental material). Both POT1a and POT1b can bind probes with the presumed natural ATC-5′ ending and the first ss nucleotide (G) next to the ds-ss junction was important for the interaction (Fig. 3A and D). When this G residue was changed to a C or base paired with the C-strand, binding was less efficient (Fig. 3A, B, and D). This result is consistent with the observation that a 12-nt GGTTAGGGTTAG probe is a better substrate

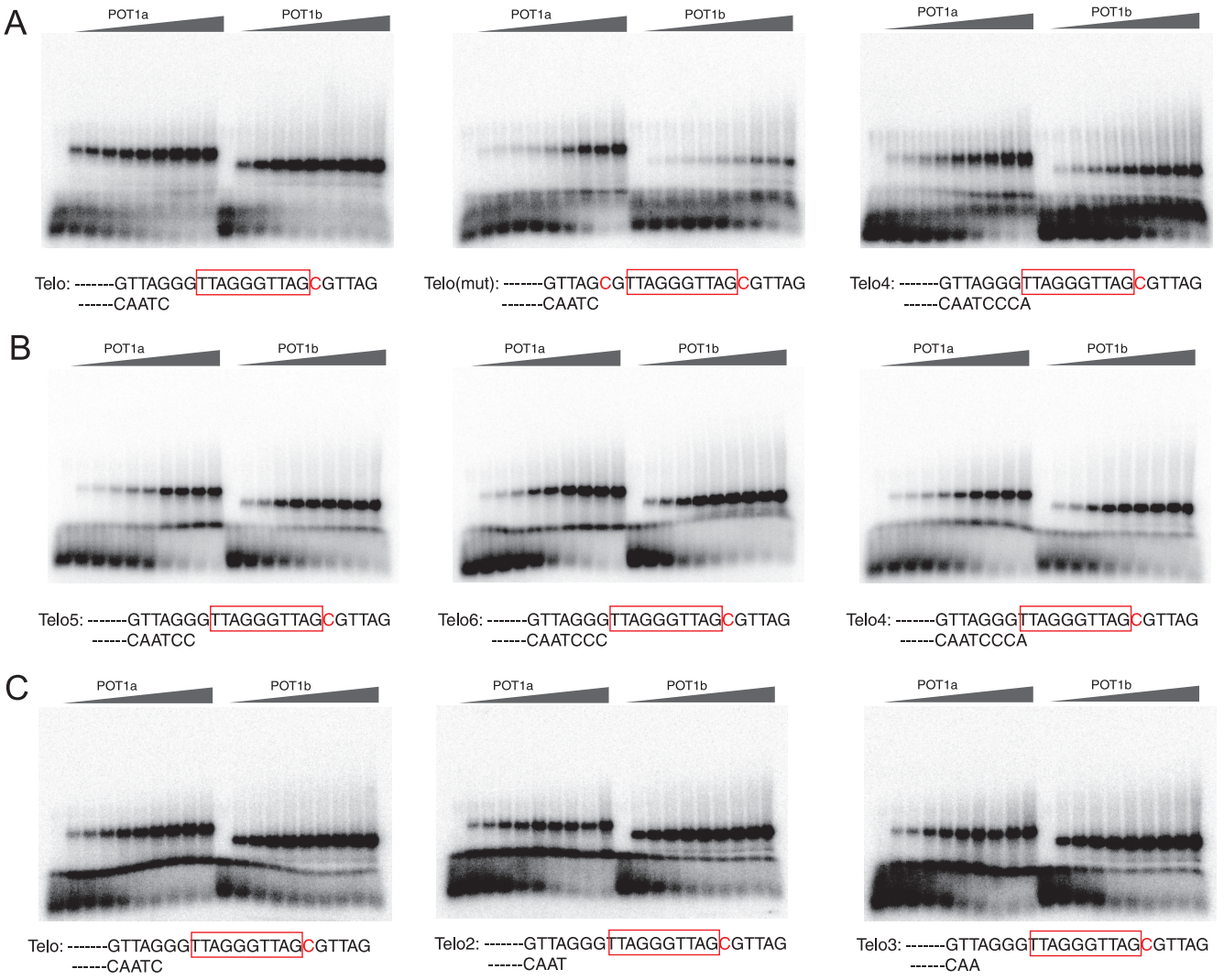

D

	Telo	Telo(mut)	Telo2	Telo3	Telo4	Telo5	Telo6
POT1a	0.8 ±0.5	3.2 ±1.9	1.9, 0.6	1.2, 0.9	2.1 ±0.7	2.3 ±1.0	2.2 ±1.1
POT1b	0.3 ±0.1	3.5 ±0.2	0.2, 0.2	0.1, 0.2	1.8 ±2.5	0.7 ±0.3	0.7 ±0.1
	GGGT C	GCGT C	AGGGT T	TAGGGT A	GGGT CCCA	GGGT CC	GGGT CCC

FIG. 3. Both POT1a and -b bind equally to telomeric ds-ss junctions. (A to C) Binding of POT1a and -b to an ss telomeric site near a ds-ss junction. The probes were incubated with increasing POT1a and -b concentrations (0.156 to 40 nM) for 30 min. Sequences of the ds-ss regions of the probes are indicated below the gels; their sequences are given in Fig. S1 in the supplemental material. All probes have a sequence change in the 3′ end blocking binding to the 3′ end. (A) Diminished binding to mutant telomere [Telo(mut)] and telomere 4 (Telo4) (shown below the gels) in which the G residue 5′ of the site is altered or base paired. (B) Diminished binding of POT1a and -b to additional probes with ds DNA next to the binding site occluding the G residues 5′ of the binding site. (C) No diminished binding to probes with available G residues 5′ of the binding site. The gel shifts shown are representatives of three independent experiments. (D) Summary of the K_d values (nM) of POT1a and POT1b in gel-shift experiments with the indicated probes. Values derived from three or more experiments are given as averages with standard deviations. Where probes were tested only twice, both values are given. All experiments were done with POT1a and -b in parallel, and K_d values were derived from quantitative analysis of phosphorimager data as shown in panels A to C.

for POT1a and POT1b than a 10-nt probe lacking the 5′ GG (9). POT1a and POT1b did not appear to recognize the ds-ss junction, since probes ending on AAT-5′ and CAA-5′ were recognized as effectively as the ATC-5′ probes (Fig. 3C and D). Thus, assuming that mouse telomeres end the same way human telomeres do, POT1a and POT1b can bind the natural structure of the telomere terminus in which the binding site immediately flanks the ds-ss junction. However, they are im-

paired in binding at the junction if the 5′ end has the sequence TCC-5′, CCC-5′, or CCA-5′, presumably due to a requirement for unpaired nucleotides immediately 5′ of the POT1 binding site. POT1a and -b did not reveal striking differences in their interactions with the ds-ss probes except that POT1a appeared slightly impaired in its binding to probes with junctions further from its binding site (Fig. 3C and D, Telo2 and Telo3). Further biochemical and structural analysis of POT1a and -b in conjunction with TPP1 and TIN2 may shed light on whether these two forms of POT1 have significant distinctions in their interactions with DNA.

Chimeras of human POT1, POT1a, and POT1b. As the biochemical analysis did not reveal an obvious difference that might explain the distinct functions of POT1a and POT1b, we took a domain-swapping approach to map the regions responsible for their differences. We included human POT1 in this approach. Ten chimeras were created carrying the DNA binding domain of one POT1 protein and the C terminus of another (Fig. 4A; see also Fig. S2 in the supplemental material). The nomenclature refers to the origin of the DNA binding domain first and to the source of the C terminus second. For example, BH has the N terminus of POT1b linked to the C terminus of human POT1. The chimeras were generated at either position 344 (350 in mouse POT1a and -b) or position 299 (301 and 300 in POT1a and -b, respectively) in the human protein. The latter chimeras are referred to as AB2, AH2, HA2, and HB2. Each of the chimeras had an N-terminal myc tag such that immunoblots with the myc antibody could be used to evaluate their relative expression levels in MEFs (Fig. 4B and C; see also Fig. S3 in the supplemental material). All chimeras were detectable, but chimeras containing sequences derived from POT1a were generally more abundant. The expression level of POT1b was invariably low. The expression level of human POT1 and chimeras containing the human POT1 C terminus were also low, but in this case, the coexpression of hTPP1 stabilized the protein, resulting in an expression level comparable to that of POT1a (Fig. 4C). The improved expression of human POT1 (or chimeras with the human C terminus) by coexpression with TPP1 is in agreement with previous data (12, 26).

All chimeras had the ability to localize to telomeres as deduced from IF analysis for colocalization of the myc-tag signals with TRF1 (Fig. 4D). For the chimeras containing the C terminus of human POT1, coexpression with hTPP1 was required for telomeric localization (Fig. 4D and data not shown).

Deletion of both POT1a and -b results in diminished proliferation of MEFs even if they are transformed with SV40-large T. Previous data indicated that either POT1a or POT1b were sufficient to sustain normal proliferation. In agreement, all POT1a/b chimeras were able to rescue the proliferation defect of DKO cells (Fig. 5). Expression of POT1b alone was slightly less effective in this regard, probably owing to the low expression level (Fig. 5E and 4B). Human POT1 and all chimeras containing human POT1 sequences also rescued the growth defect, provided that hTPP1 was present for those proteins containing the C terminus of human POT1.

Repression of ATR signaling depends on the DNA binding domain. Previous data showed that POT1a and POT1b differ in their ability to repress DNA damage signaling at telomeres, POT1b being less effective than POT1a. Human POT1, when provided with hTPP1, was equally as effective as POT1a in repressing the occurrence of TIFs at the chromosome ends of POT1 DKO cells (10, 12). We tested the chimeric proteins for their capacity to repress the DNA damage response by monitoring the formation of γ-H2AX and 53BP1 foci at telomeres (Fig. 6A; see also Fig. S4 in the supplemental material). No telomeric γ-H2AX or 53BP1 foci occurred in the POT1 DKO cells before treatment with Cre (data not shown), indicating that none of the proteins acted as a dominant-negative allele. As expected, Cre-treated POT1 DKO cells containing POT1a or human POT1 showed a strong reduction in the incidence of TIFs compared to the vector control (Fig. 6A). When POT1a or human POT1 were present, less than 20% of the Cre-treated DKO cells contained more than 10 TIFs. The HA chimera and the AH chimera combined with hTPP1 were also effective in protecting the telomeres from ATR signaling. In addition, chimeras containing the C terminus of POT1b and the DNA binding domain of POT1a or human POT1 were effective in telomere protection. In contrast, all chimeras containing the DNA binding domain of POT1b were much less capable of repressing the ATR pathway (Fig. 6A). This difference was not due to diminished expression levels. For instance, AH and BH are expressed at the same level (Fig. 4C and data not shown), but only the former reduces the TIF response to near the background level. Similarly, BA is expressed at a higher level than HB, yet the cells show a stronger TIF response. Furthermore, in cells expressing BH together with hTPP1, there were 53BP1 foci at telomeres that contained both hTPP1 and the BH chimera (see Fig. S4 in the supplemental material). These data indicate that the ability of POT1 proteins to repress ATR signaling is in part a feature of their DNA binding domains (Fig. 6B). OB1 and OB2 of human POT1 and POT1a are efficient repressors of ATR signaling, regardless of the C terminus of the chimeras. The N terminus of POT1b, while not completely deficient in this attribute, is less potent as a repressor of ATR signaling.

The C terminus of POT1b specifies its ability to limit 5′-end resection. In the absence of POT1b, telomeres shorten faster and carry excessively long 3′ overhangs (10, 11). Previous data had shown that POT1b, but not POT1a or human POT1, can block this inappropriate processing of the telomere terminus (12). We tested all chimeras to map the domains in POT1b responsible for this attribute. Chimeric proteins were introduced into conditional POT1b cells ($POT1b^{S/F}$), and the change in the 3′-end structure was monitored by in-gel analysis 5 to 6 days after the deletion of POT1b (Fig. 7; see also Fig. S5 and S6 in the supplemental material). In addition, the chimeras were introduced into POT1 DKO cells, and the assay was repeated in the absence of both endogenous POT1 proteins (see Fig. S5 in the supplemental material). The data are summarized in Fig. 8.

As expected, POT1b but not POT1a or a mutant of POT1b that lacks DNA binding activity (F62A [7; data not shown]), restored the ability of cells to maintain the normal structure of the telomere terminus. The only POT1a/b chimera that shared this ability with full-length POT1b was AB2. Variations in the expression of the chimeric proteins did not appear relevant since POT1b is fully proficient at repressing 5′-end resection while being expressed at the lowest level of all introduced proteins. Therefore, the difference between POT1a and

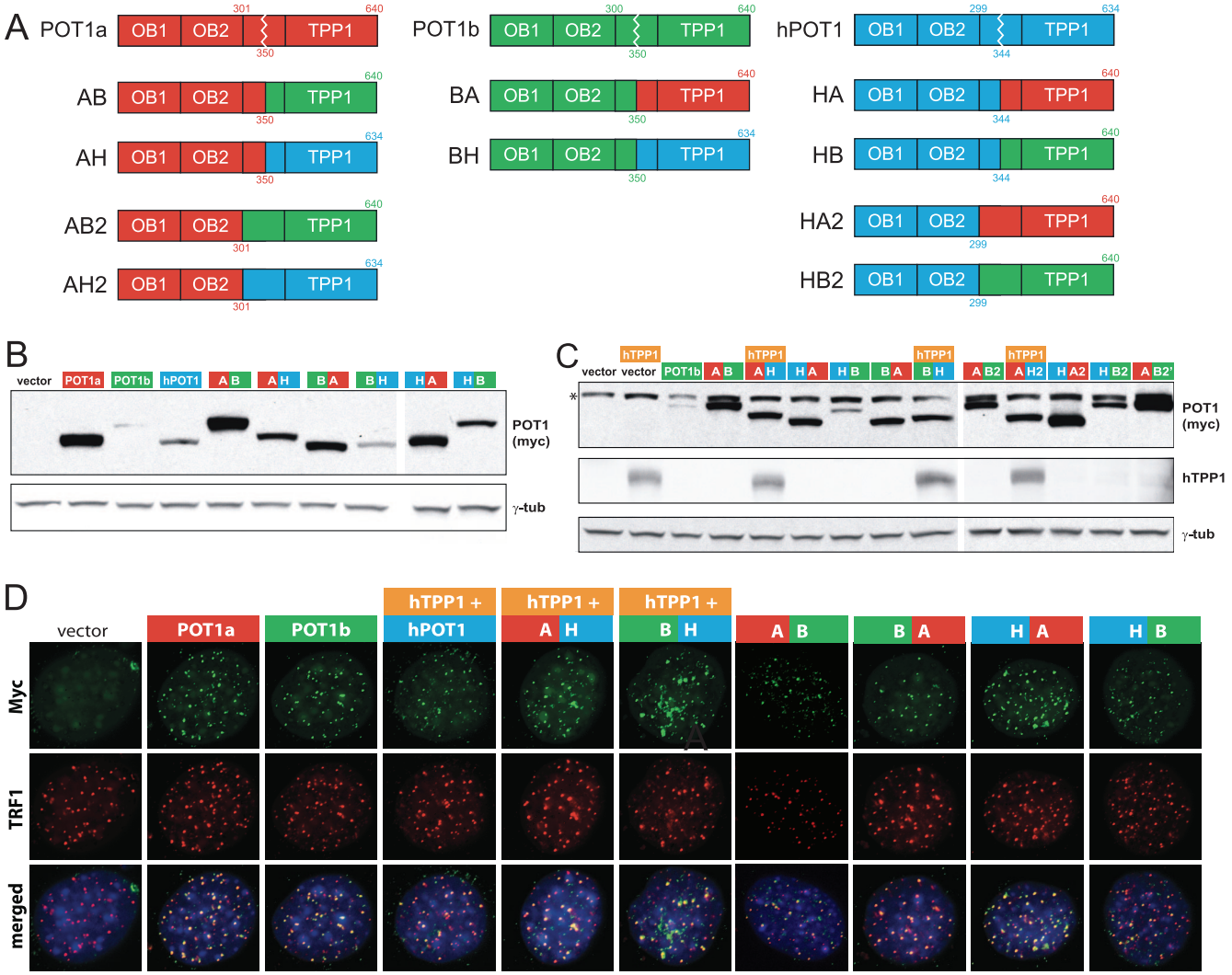

FIG. 4. Structure, expression, and localization of POT1 chimeras. (A) POT1a, POT1b, and human POT1 (hPOT1) were divided into N- and C-terminal parts between the second OB fold of the DNA binding domain and the TPP1 interaction domain and fused together according to the six possible permutations. In the schematic depiction, red corresponds to POT1a, green to POT1b, and blue to human POT1. For one set of POT1 chimeras (AB, AH, BA, BH, HA, and HB), the swapping of the domains takes place at aa 350 (POT1a and POT1b) or aa 344 (human POT1). The domain swap of a second set of chimeras (AB2, AH2, HA2, and HB2) takes place at the very end of the second OB fold at aa 301 (POT1a) and aa 299 (human POT1). (B) Immunoblot on cells expressing POT1a, POT1b, human POT1, or POT1 chimeras. MEFs conditionally targeted for POT1a and POT1b ($POT1a^{S/F}$ $POT1b^{S/F}$) were infected with pWZL-N-myc-POT1 or vector (pWZL) and cell extracts prepared after hygromycin selection. (C) Immunoblot on cells expressing POT1b or POT1 chimeras and if indicated hTPP1. MEFs conditionally targeted for POT1b ($POT1b^{S/F}$) were infected with pWZL-N-myc-POT1 or vector (pWZL) and selected with hygromycin. Cells were then infected with pLPC-N-flag-hTPP1 or vector (pLPC), and cell extracts prepared after puromycin selection. AB2′-expressing cells represent an independent infection of $POT1b^{S/F}$ MEFs with AB2. The asterisk indicates a nonspecific band. (D) IF on cells expressing POT1a, POT1b, human POT1, or chimeric POT1 proteins. hTPP1 was introduced into the $POT1a^{S/F}$ $POT1b^{S/F}$ MEFs depicted in panel B that were expressing POT1 constructs with the C terminus of human POT1; otherwise, cells were infected with empty vector (pLPC). Endogenous POT1a and POT1b were deleted with adenoviral Cre. Cells were analyzed by IF for the myc epitope tag of the POT1 variants (green) and TRF1 (red) and counterstained with DAPI (4′,6-diamidino-2-phenylindole; blue). Similar results were obtained for wild-type cells (data not shown), but the telomeric accumulation of ectopic POT1 variants in the presence of endogenous POT1 was lower overall. Antibodies used for the experiments depicted in panels B to D are 9E10 for myc, M2 for Flag, 644 for TRF1, 1151 for TPP1, and GTU88 for γ-tubulin (γ-tub).

POT1b resides in the C-terminal half of the protein. As chimera AB is much less effective than AB2 in repressing 5′-end resection, a region between positions 300 and 350 is relevant to this function. In agreement with the importance of the C-terminal half of POT1b for the regulation of the telomere terminus, a chimeric protein bearing the POT1b OB folds and the C terminus of POT1a (BA) acted as a dominant-negative allele in several experiments (Fig. 8; see Fig. S5 in the supplemental material), inducing an increase in the 3′-overhang signal even when endogenous POT1b was present.

Chimeras containing the POT1b C terminus and the N terminus of human POT1 were also capable of restoring normal overhang metabolism. Both HB and HB2 were effective, indicating that the 300 to 350 domain of POT1b needed for this

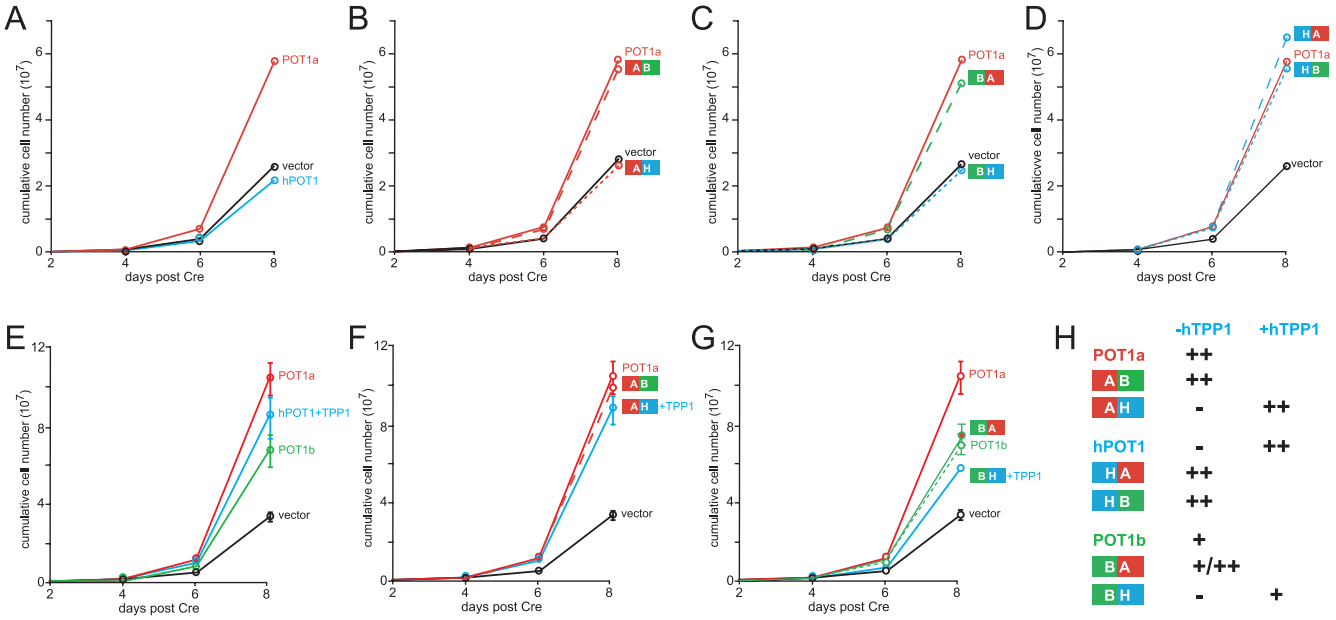

FIG. 5. Chimeric POT1 proteins suppress the growth defects of POT1a and POT1b DKO cells. Growth curves of MEFs conditionally targeted for both POT1a and POT1b ($POT1a^{S/F}$ $POT1b^{S/F}$) expressing the different POT1 variants and, if indicated, hTPP1 after the deletion of endogenous POT1a and POT1b with adenoviral Cre. The growth curves depicted in panels A to D were acquired in parallel and in duplicate; the growth curves depicted in panels E to G were acquired in parallel and in triplicate. (H) Summary of the capability of human and mouse POT1 proteins and their chimeras to rescue cell proliferation in POT1a and POT1b DKO MEFs. ++, efficient suppression of growth defects (comparable to POT1a); +, partial suppression of growth defects; −, no suppression of growth defects.

function can be replaced by the human counterpart. As noted above for BA, HA and HA2 often had a dominant-negative effect, increasing the overhang signal in the presence of the endogenous POT1b (Fig. 7 and 8; see also Fig. S5 in the supplemental material). Thus, human POT1 contains one of the two POT1b-specific determinants of telomere terminus processing.

DISCUSSION

In contrast to humans and other mammals, rodents contain two functionally distinct POT1 proteins as a result of a gene duplication. Among the mammalian genes involved in basic genome maintenance, such variation is unusual, warranting the current study on the similarities and distinctions between the mouse POT1 genes on the one hand, and the human gene on the other. Furthermore, definition of the similarities and differences of the mouse and human POT1 proteins is crucial for attempts to model human telomere biology and telomere-based diseases in mice.

Prior to this work, two functional domains were recognized in POT1: an N-terminal DNA binding domain and a C-terminal TPP1 interaction domain that serves to target POT1 to telomeres. Previous data had shown that POT1a and POT1b show no overt differences in their interaction with TPP1 (9, 12), and the data reported here do not reveal substantial differences in the DNA binding features of POT1a and POT1b. In particular, POT1a and POT1b bind equally well to their recognition site at a 3′ end, at a 5′ end, and when positioned near an ss-ds junction, suggesting that both proteins can bind all along the 3′ overhang and to ss telomeric DNA in a D loop. Despite these results, we consider it possible that POT1a and POT1b are dissimilar in some aspect of their interaction with DNA that is not probed by the in vitro studies presented here.

The differences between POT1a, POT1b, and human POT1 were, however, revealed by a domain-swapping approach. The experiments showed that the nature of the N terminus of POT1 determines its capacity to repress ATR activation: chimeras with the N terminus of POT1a or human POT1 completely suppress the DNA damage response in mouse cells from which the endogenous POT1 proteins are deleted. In contrast, chimeras with the POT1b N terminus only partially protect telomeres from a DNA damage response, similarly to POT1b. The C termini of POT1a, POT1b, and human POT1 are functionally equivalent in terms of the repression of ATR activation at telomeres, acting mainly as a recruitment domain by interacting with TPP1 and thus mediating the association of POT1 with the rest of shelterin. Given the lack of differences in the DNA binding features of POT1a and POT1b, an aspect of the N-terminal domain other than 3′-overhang binding may contribute to ATR repression. Alternatively, the two proteins may have different DNA binding features when associated with the other shelterin components. For instance, recent work showed that hTPP1 improves the affinity of human POT1 for its DNA substrate (26); therefore, mouse TPP1 might modulate the DNA binding properties of POT1a and POT1b in distinct ways. It has been proposed that POT1 inhibits ATR activation by blocking the access of RPA to the 3′ overhang (12, 16). According to this model, the only prerequisite for POT1 to inhibit a DNA damage signal at telomeres is its ability to bind the telomeric overhang with a higher affinity than that of RPA. Although POT1a and POT1b do not differ in their

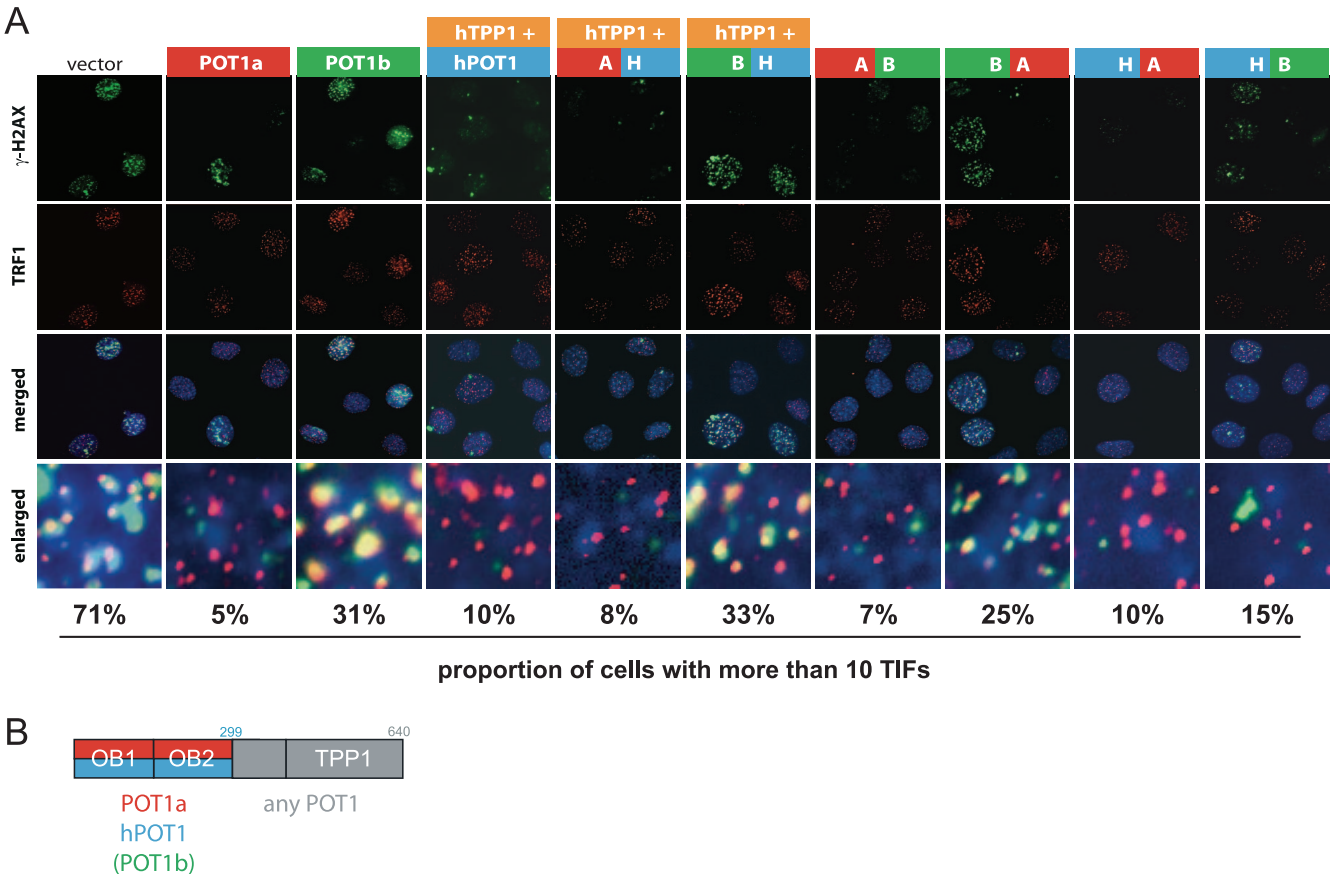

FIG. 6. The DNA binding domains of POT1a or human POT1 repress ATR signaling. (A) MEFs conditionally targeted for POT1a and POT1b ($POT1a^{S/F}$ $POT1b^{S/F}$) expressing the different POT1 variants and, if indicated, hTPP1 were infected with adenoviral Cre. Four days after the application of Cre, the occurrence of TIFs was monitored by IF for γ-H2AX (green) and TRF1 (red), and counterstained with DAPI (4′,6-diamidino-2-phenylindole; blue). The growth curves depicted in Fig. 5E to G were obtained from the same set of Cre-infected cells. (B) Schematic representation of the POT1 chimeras that can repress ATR signaling. Chimeric proteins with the DNA binding domain of POT1a or human POT1 efficiently suppress TIF formation; the DNA binding domain of POT1b can do so but to a minor extent. The provenance of the C terminus is not critical in this regard, although POT1 variants with the human C terminus require the coexpression of hTPP1 for telomeric localization.

affinity and specificity for ss telomeric DNA, POT1a may prevent RPA binding to the 3′ overhang through a different mechanism.

The domain-swapping experiments also revealed a critical role of the POT1b C terminus for the protection of mouse telomeres from excessive 5′-end resection. POT1 chimeras with the POT1b C terminus and any DNA binding domain of the human or mouse POT1 proteins can complement the loss of endogenous POT1b, while chimeras with the POT1a or human POT1 C terminus fail to do so. The simplest explanation for these findings is a novel domain in the C terminus of POT1b, which is not conserved in POT1a. The location of this domain was deduced based on chimeras that differ in a region between the DNA binding and the TPP1 interaction domain from amino acids (aa) 300 to 350. Our data show that this domain is critical for POT1b function, and while its molecular properties are as yet undetermined, we envision that it might be an interface for the interaction with either an unknown protein or telomeric DNA. Through this novel domain, POT1b conceivably regulates or inhibits the putative nuclease involved in 5′-end resection, or another factor upstream in the pathway, which regulates this nuclease. However, a two-hybrid screen with POT1b did not reveal POT1b-specific interaction partners (W. Palm, T. Kibe, and T. de Lange, unpublished data). Human POT1 and POT1b are functionally equivalent in the region between aa 300 to 350, as both HB and HB2 can substitute for POT1b, revealing a partial functional conservation of POT1b and human POT1, but not POT1a, with regard to the regulation of 5′-end resection. Human POT1 sequences do not have the ability to replace the second C-terminal domain of POT1b needed for the proper structure of the telomere terminus. The basis for this distinction may lie in human POT1 itself or its interaction with other shelterin components.

The data presented here allow for the drawing of first conclusions in terms of the functional divergence of POT1a and POT1b and their evolutionary relationships to human POT1. It is reasonable to assume that a duplication of the ancestral mammalian POT1 gene in rodents alleviated the selection pressure to retain all of the functions required of telomeric 3′-overhang binding proteins in both copies of POT1. Because ATR activation at telomeres is completely repressed by POT1a, it was possible for POT1b to lose this function. On the other hand, POT1a is not required to regulate the terminal chromosome structure, as POT1b executes this task. The du-

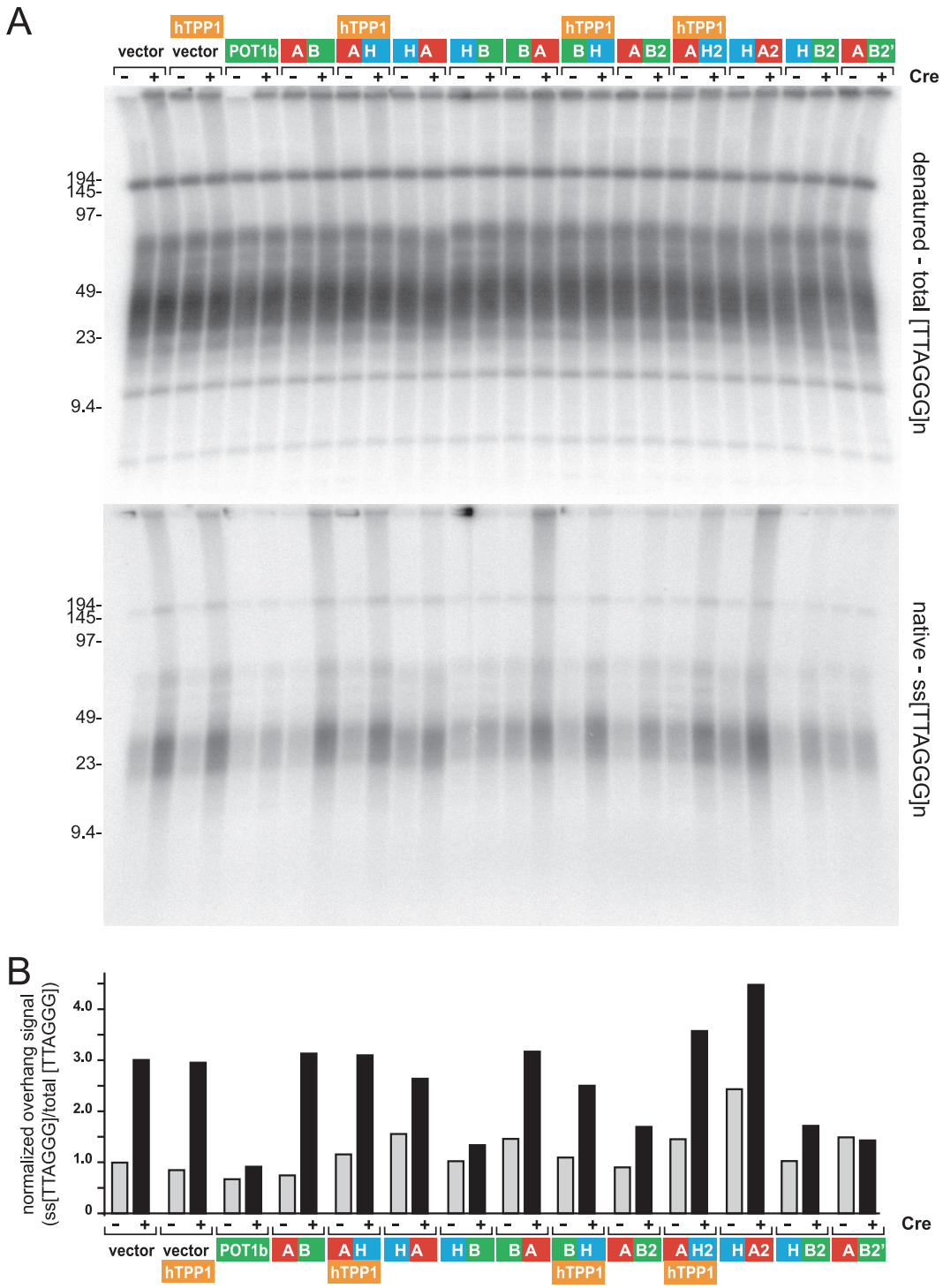

FIG. 7. The POT1b C terminus is required to control 5′-end resection. (A) In-gel overhang assay of MEFs conditionally targeted for POT1b (POT1b$^{S/F}$) expressing POT1b or POT1 chimeras. Cells were retrovirally transduced with the indicated POT1 variants in pWZL-N-myc or vector control (pWZL) and selected with hygromycin. Subsequently, cells were infected with pLPC-N-flag-hTPP1 or vector (pLPC) and selected with puromycin. POT1b was deleted using Hit&Run Cre, and overhang length was determined 6 days after the application of Cre. (B) Quantification of the overhang signals of the cells depicted in panel A. AB2′-expressing cells represent an independent infection of POT1b$^{S/F}$ MEFs with AB2.

plication of the POT1 gene may also have facilitated the acquisition of new functions by one of the two POT1 orthologs.

Whereas POT1a and POT1b have diverged sufficiently to differ in their ability to control ATR signaling and 5′-end resection, our data indicate that both proteins are capable of controlling HDR at telomeres. POT1a and POT1b prevent HDR in parallel with Ku70 and are functionally equivalent in this regard: the simultaneous deletion of POT1a and POT1b

FIG. 8. Summary of the ability of the indicated POT1 chimeras to prevent the inappropriate resection of the telomeric 5′ end in the absence of POT1b. Results of the overhang assays are shown in Fig. 7 and in Fig. S5 in the supplemental material. For chimeras containing the C terminus of human POT1, hTPP1 was coexpressed in some experiments as indicated. +, repression of the increase in the overhang signal after the deletion of POT1b; −, minimal or no repression of the overhang signal; DN, no rescue of the overhang signal increase after the deletion of POT1b, combined with an increase in the overhang signal in cells containing POT1b. The asterisks indicate experiments in which human POT1 was not localized to telomeres due to the absence of hTPP1.

from Ku70$^{-/-}$ cells leads to an elevated frequency of T-SCEs, whereas the presence of any of the three proteins at telomeres grants full protection from HDR. The T-SCE rate of POT1 DKO cells deficient for Ku70 is comparable to the T-SCE rate of cells deficient for TRF2 and Ku70. It remains to be determined whether the role of TRF2 in this pathway is simply to recruit POT1a or POT1b. We note that POT1 and TRF2 block HDR at telomeres to a similar extent, whereas the nonhomologous end joining of telomeres is primarily suppressed by TRF2, with POT1 being largely dispensable in this regard (2, 3, 10).

Our studies indicate that human POT1 combines specific attributes of POT1a and POT1b. Human POT1 can repress ATR signaling when positioned at mouse telomeres and has one of the regions required for regulation of the 5′-end resection of POT1. The fact that human POT1 defines the 5′ end of human telomeres suggests that a POT1b-like function indeed

exists in human POT1 and that 5′-end resection in human cells may also be limited by POT1. This conclusion is relevant to human disease states that involve shortened telomeres such as dyskeratosis congenita (reviewed in reference 6). The enhanced telomere shortening associated with POT1b deficiency in mice results in phenotypes resembling dyskeratosis congenita (11). The demonstration that human POT1 shares a critical domain with POT1b suggests that mutations in human POT1 that affect this function could also lead to inappropriate telomere shortening. An examination of the POT1 gene in cases of dyskeratosis congenita with no known genetic basis may therefore be prudent.

ACKNOWLEDGMENTS

We thank Devon White for expert mouse husbandry and members of the de Lange lab for comments on the manuscript. Eros Lazzerini Denchi is thanked for providing instruction in CO-FISH.

This work was supported by grants from the NIH (CA76027, GM049046, and AG016642) to T.D.L. W.P. was supported by the Studienstiftung des deutschen Volkes. D.H. was supported by a Cancer Research Institute Predoctoral Emphasis Pathway in Tumor Immunology grant and Rockefeller University graduate program funds. T.K. was supported as a research fellow by the Japan Society for the promotion of Science and the Toyobo Biotechnology Foundation.

REFERENCES

1. **Baumann, P., and T. R. Cech.** 2001. Pot1, the putative telomere end-binding protein in fission yeast and humans. Science **292:**1171–1175.
2. **Celli, G., and T. de Lange.** 2005. DNA processing not required for ATM-mediated telomere damage response after TRF2 deletion. Nat. Cell Biol. **7:**712–718.
3. **Celli, G. B., E. Lazzerini Denchi, and T. de Lange.** 2006. Ku70 stimulates fusion of dysfunctional telomeres yet protects chromosome ends from homologous recombination. Nat. Cell Biol. **8:**885–890.
4. **Churikov, D., and C. M. Price.** 2008. Pot1 and cell cycle progression cooperate in telomere length regulation. Nat. Struct. Mol. Biol. **15:**79–84.
5. **de Lange, T.** 2005. Shelterin: the protein complex that shapes and safeguards human telomeres. Genes Dev. **19:**2100–2110.
6. **Dokal, I., and T. Vulliamy.** 2005. Telomerase deficiency and human disease, p. 139–162. *In* T. de Lange, V. Lundblad, and E. Blackburn (ed.), Telomeres. Cold Spring Harbor Laboratory Press, Cold Spring Harbor, NY.
7. **Gottschling, D. E., and V. A. Zakian.** 1986. Telomere proteins: specific recognition and protection of the natural termini of Oxytricha macronuclear DNA. Cell **47:**195–205.
8. **Griffith, J. D., L. Comeau, S. Rosenfield, R. M. Stansel, A. Bianchi, H. Moss, and T. de Lange.** 1999. Mammalian telomeres end in a large duplex loop. Cell **97:**503–514.
9. **He, H., A. S. Multani, W. Cosme-Blanco, H. Tahara, J. Ma, S. Pathak, Y. Deng, and S. Chang.** 2006. POT1b protects telomeres from end-to-end chromosomal fusions and aberrant homologous recombination. EMBO J. **25:**5180–5190.
10. **Hockemeyer, D., J. P. Daniels, H. Takai, and T. de Lange.** 2006. Recent expansion of the telomeric complex in rodents: two distinct POT1 proteins protect mouse telomeres. Cell **126:**63–77.
11. **Hockemeyer, D., W. Palm, R. C. Wang, S. S. Couto, and T. de Lange.** 2008. Engineered telomere degradation models dyskeratosis congenita. Genes Dev. **22:**1773–1785.
12. **Hockemeyer, D., W. Palm, T. Else, J. P. Daniels, K. K. Takai, J. Z. Ye, C. E. Keegan, T. de Lange, and G. D. Hammer.** 2007. Telomere protection by mammalian POT1 requires interaction with TPP1. Nat. Struct. Mol. Biol. **14:**754–761.
13. **Hockemeyer, D., A. J. Sfeir, J. W. Shay, W. E. Wright, and T. de Lange.** 2005. POT1 protects telomeres from a transient DNA damage response and determines how human chromosomes end. EMBO J. **24:**2667–2678.
14. **Houghtaling, B. R., L. Cuttonaro, W. Chang, and S. Smith.** 2004. A dynamic molecular link between the telomere length regulator TRF1 and the chromosome end protector TRF2. Curr. Biol. **14:**1621–1631.
15. **Karlseder, J., D. Broccoli, Y. Dai, S. Hardy, and T. de Lange.** 1999. p53- and ATM-dependent apoptosis induced by telomeres lacking TRF2. Science **283:**1321–1325.
16. **Lazzerini Denchi, E., and T. de Lange.** 2007. Protection of telomeres through independent control of ATM and ATR by TRF2 and POT1. Nature **448:**1068–1071.
17. **Lei, M., E. R. Podell, and T. R. Cech.** 2004. Structure of human POT1 bound to telomeric single-stranded DNA provides a model for chromosome end-protection. Nat. Struct. Mol. Biol. **11:**1223–1229.
18. **Lei, M., A. J. Zaug, E. R. Podell, and T. R. Cech.** 2005. Switching human telomerase on and off with hPOT1 protein in vitro. J. Biol. Chem. **280:**20449–20456.
19. **Liu, D., A. Safari, M. S. O'Connor, D. W. Chan, A. Laegeler, J. Qin, and Z. Songyang.** 2004. PTOP interacts with POT1 and regulates its localization to telomeres. Nat. Cell Biol. **6:**673–680.
20. **Palm, W., and T. de Lange.** 2008. How shelterin protects mammalian telomeres. Annu. Rev. Genet. **42:**301–334.
21. **Raices, M., R. E. Verdun, S. A. Compton, C. I. Haggblom, J. D. Griffith, A. Dillin, and J. Karlseder.** 2008. C. elegans telomeres contain G-strand and C-strand overhangs that are bound by distinct proteins. Cell **132:**745–757.
22. **Sfeir, A. J., W. Chai, J. W. Shay, and W. E. Wright.** 2005. Telomere-end processing the terminal nucleotides of human chromosomes. Mol. Cell **18:**131–138.
23. **Shakirov, E. V., Y. V. Surovtseva, N. Osbun, and D. E. Shippen.** 2005. The *Arabidopsis* Pot1 and Pot2 proteins function in telomere length homeostasis and chromosome end protection. Mol. Cell. Biol. **25:**7725–7733.
24. **van Steensel, B., A. Smogorzewska, and T. de Lange.** 1998. TRF2 protects human telomeres from end-to-end fusions. Cell **92:**401–413.
25. **Veldman, T., K. T. Etheridge, and C. M. Counter.** 2004. Loss of hPot1 function leads to telomere instability and a cut-like phenotype. Curr. Biol. **14:**2264–2270.
26. **Wang, F., E. R. Podell, A. J. Zaug, Y. Yang, P. Baciu, T. R. Cech, and M. Lei.** 2007. The POT1-TPP1 telomere complex is a telomerase processivity factor. Nature **445:**506–510.
27. **Wang, R. C., A. Smogorzewska, and T. de Lange.** 2004. Homologous recombination generates T-loop-sized deletions at human telomeres. Cell **119:**355–368.
28. **Wei, C., and C. M. Price.** 2004. Cell cycle localization, dimerization, and binding domain architecture of the telomere protein cPot1. Mol. Cell. Biol. **24:**2091–2102.
29. **Wu, L., A. S. Multani, H. He, W. Cosme-Blanco, Y. Deng, J. M. Deng, O. Bachilo, S. Pathak, H. Tahara, S. M. Bailey, Y. Deng, R. R. Behringer, and S. Chang.** 2006. Pot1 deficiency initiates DNA damage checkpoint activation and aberrant homologous recombination at telomeres. Cell **126:**49–62.
30. **Ye, J. Z., D. Hockemeyer, A. N. Krutchinsky, D. Loayza, S. M. Hooper, B. T. Chait, and T. de Lange.** 2004. POT1-interacting protein PIP1: a telomere length regulator that recruits POT1 to the TIN2/TRF1 complex. Genes Dev. **18:**1649–1654.

SUPPLEMENTAL FIGURES

Supplemental Figure 1. Palm et al.

Supplemental Figure 1. DNA probes used for the biochemical analysis of POT1a and POT1b.
Schematic of POT1 probes Telo, Telo(mut), Telo2, Telo3, Telo4, Telo5, and Telo6. The red letters nucleotide changes in the POT1 recognition sites; the minimal binding site of POT1 is indicated by red boxes. EcoRI restriction sites were inserted in duplex region to confirm that labelled oligos are annealed correctly. The asterisks show the sequences used for labeling by Klenow fill-in.

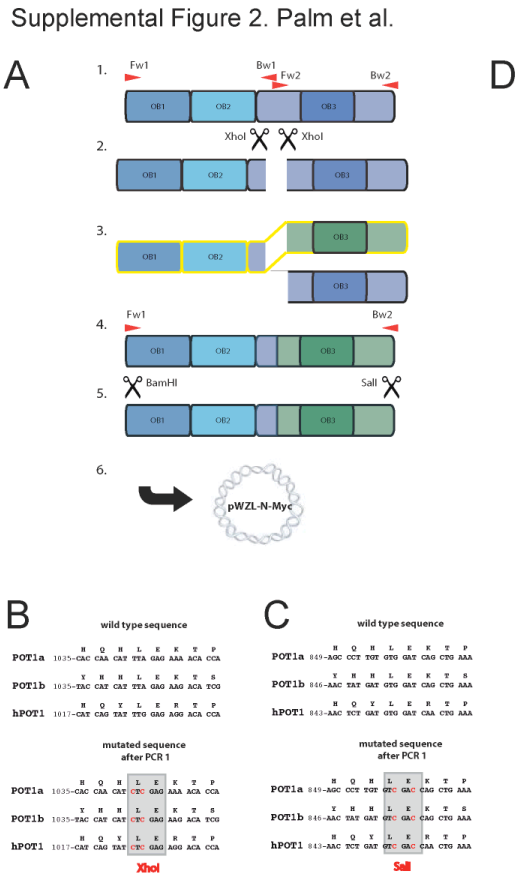

D

Name	Sequence
hPOT1 fw1	atgc ggatcc TCT TT G GTT CCA G CAA CA AAT
hPOT1 fw2	atgc ctcgag AGG ACA CCA CTA T GT GCC
hPOT1 bw1	atgc ctcgag AT A CTG AT G AT C TGT AAG TAT TGT A
hPOT1 bw2	atgc gtcgac TTA GAT TA C AT C TTC TG C A AC
hPOT1 fw2.2	atgc gtcgac CAA CTG AAA AAG GAT T TA GAA
hPOT1 bw1.2	atgc gtcgac ATC AGA GTT ACT TTC T GG CAA G
hPOT1 bw2.2	atgc ctcgag TTA GAT TA C AT C TTC TG C A AC
POT1a fw1	atgc ggatcc TCT TT G GTT TCA ACA GCT CCC
POT1a fw2	atgc ctcgag AAAA CA CCA CTG T GT GCC
POT1a bw1	atgc ctcgag ATG TTG GTG ATT GGT AAG T AT T G
POT1a bw2	atgc gtcgac CTA GAC AAC ATT TTC TG C A AC
POT1a fw2.2	atgc gtcgac CAG CT G A AA A AA GCT T TA GAA
POT1a bw1.2	atgc gtcgac ACA AGG GCT TGT ATC T GG CAA
POT1a bw2.2	atgc ctcgag CTA GAC AAC ATT TTC TG C A AC TG
POT1b fw1	atgc ggatcc TCT TC G GC C CCA G TA GCA CC
POT1b fw2	atgc ctcgag AA G A CA TC G TTG TGT GAC ATT TTG
POT1b bw1	atgc ctcgag ATG AT G GT A AC C TGT AAG TG
POT1b bw2	atgc gtcgac CTA GAT GAT GTC TT C TGC AAT C
POT1b fw2.2	atgc gtcgac CAG CT G A AA A AA GCT T TA GAA
POT1b bw1.2	atgc gtcgac ATC AT A GT T ACT TTC T GG TAA G
POT1b bw2.2	atgc ctcgag CTA GAT GAT GTC TT C TGC AAT C

Supplemental Figure 2. Cloning strategy for chimeras of POT1a, POT1b and human POT1

(A) Schematic overview of the strategy for the cloning of chimeric POT1 proteins. (1.) PCR amplification of the N- and C-terminal parts of POT1a, POT1b and human POT1. (2.) Digest of the PCR fragments with XhoI. (3.) Ligation of the N- and C-termini of different POT1 proteins in order to generate chimeras. (4.) PCR amplification of the chimeric POT1 proteins. (5.) Digest of the amplified constructs with BamHI and SalI. (6.) Insertion of the constructs into pWZL-N-myc using the N-terminal BamHI and C-terminal SalI restriction sites. (B) Changes in the wild type nucleotide sequence generated with the primers Bw1 and Fw2 that introduce the XhoI restriction site. These changes do not lead to alterations of the amino acid sequence. (C) Changes in the wild type sequence for the cloning of the second set of domain swap mutants (AB2, AH2, HA2, HB2). The primers Bw1.2 and Fw2.2 introduced a SalI restriction site, the primer Bw2.2 an XhoI site. These changes do not lead to alterations of the amino acid sequence. For the insertion into the vector, the insert was digested with BamHI and XhoI, pWZL-N-myc with BamHI and SalI. Sticky ends generated by SalI and XhoI can be ligated, leading to the destruction of the respective restriction site. (D) Primers for the generation of chimeric POT1 proteins. The primer pairs fw1, bw1 and fw2, bw2 were used for PCR amplification of the N-terminal and C-terminal parts, respectively of the different POT1 proteins. The part of each primer, which is complementary to the nucleotide sequence of the respective POT1 gene, is written in capital letters. The part of each primer written in lowercase letters contains four initial unspecific nucleotides followed by the restriction site used for subsequent insertion into the vector.

Supplemental Figure 3. Palm et al.

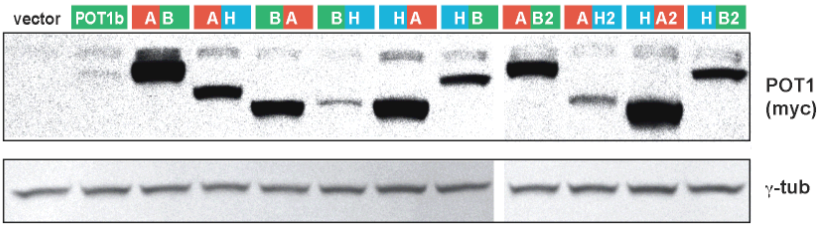

Supplemental Figure 3. Expression of POT1 chimeras in POT1b$^{S/F}$ cells

Immunoblot on cells expressing POT1b or POT1 chimeras. MEFs conditionally targeted for POT1b (POT1b$^{S/F}$) were infected with pWZL-N-myc-POT1 or vector (pWZL) and cell extracts prepared after hygromycin selection. Antibodies used are MYC (9E10), γ-tubulin (GTU88).

Supplemental Figure 4. Palm et al.

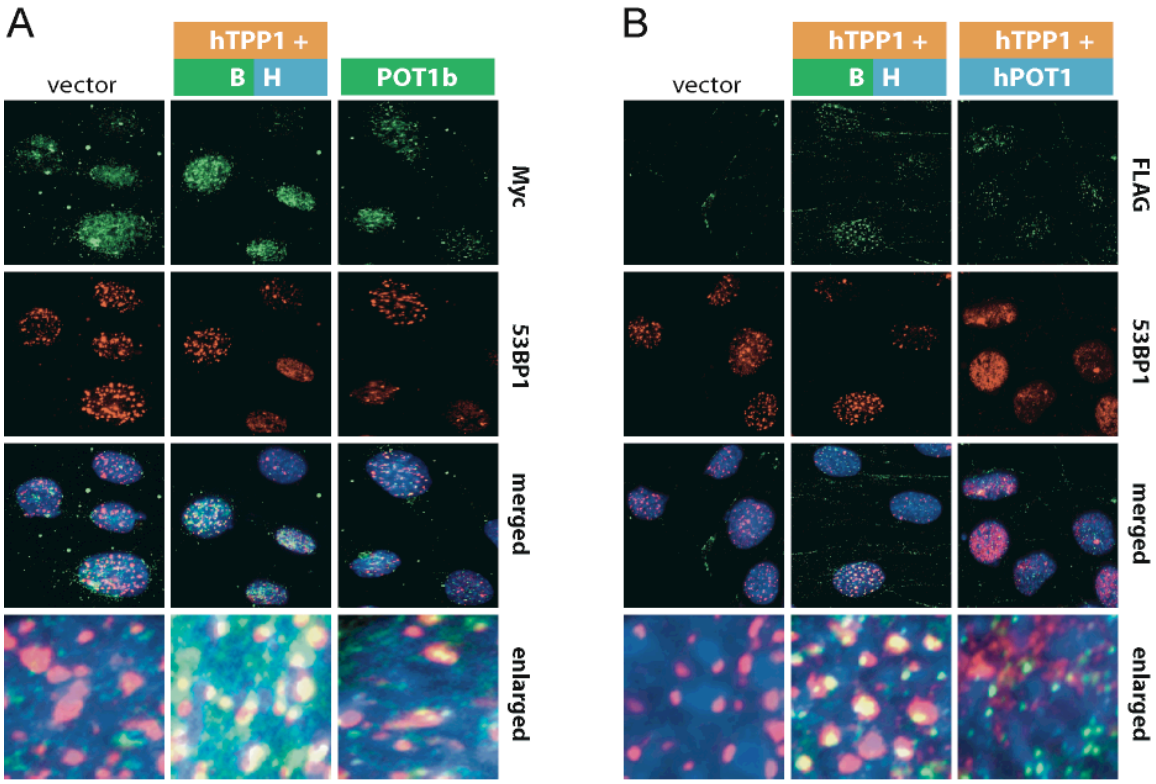

Supplemental Figure 4. POT1 variants with the POT1b N-terminus are only partially able to protect telomeres from DNA damage signaling pathways

(A) MEFs conditionally targeted for both POT1a and POT1b (POT1a$^{S/F}$ POT1b$^{S/F}$) expressing different POT1 variants and if indicated human TPP1 were infected with Hit&Run Cre. Four days after infection, cells were analyzed by IF for the myc tag of POT1 (green) and 53BP1 (red), and counter stained with DAPI (blue). (B) Cells described in (A) were analyzed by IF for the flag tag of TPP1 (green) and 53BP1 (red), and counter stained with DAPI (blue).

Supplemental Figure 5. Palm et al.

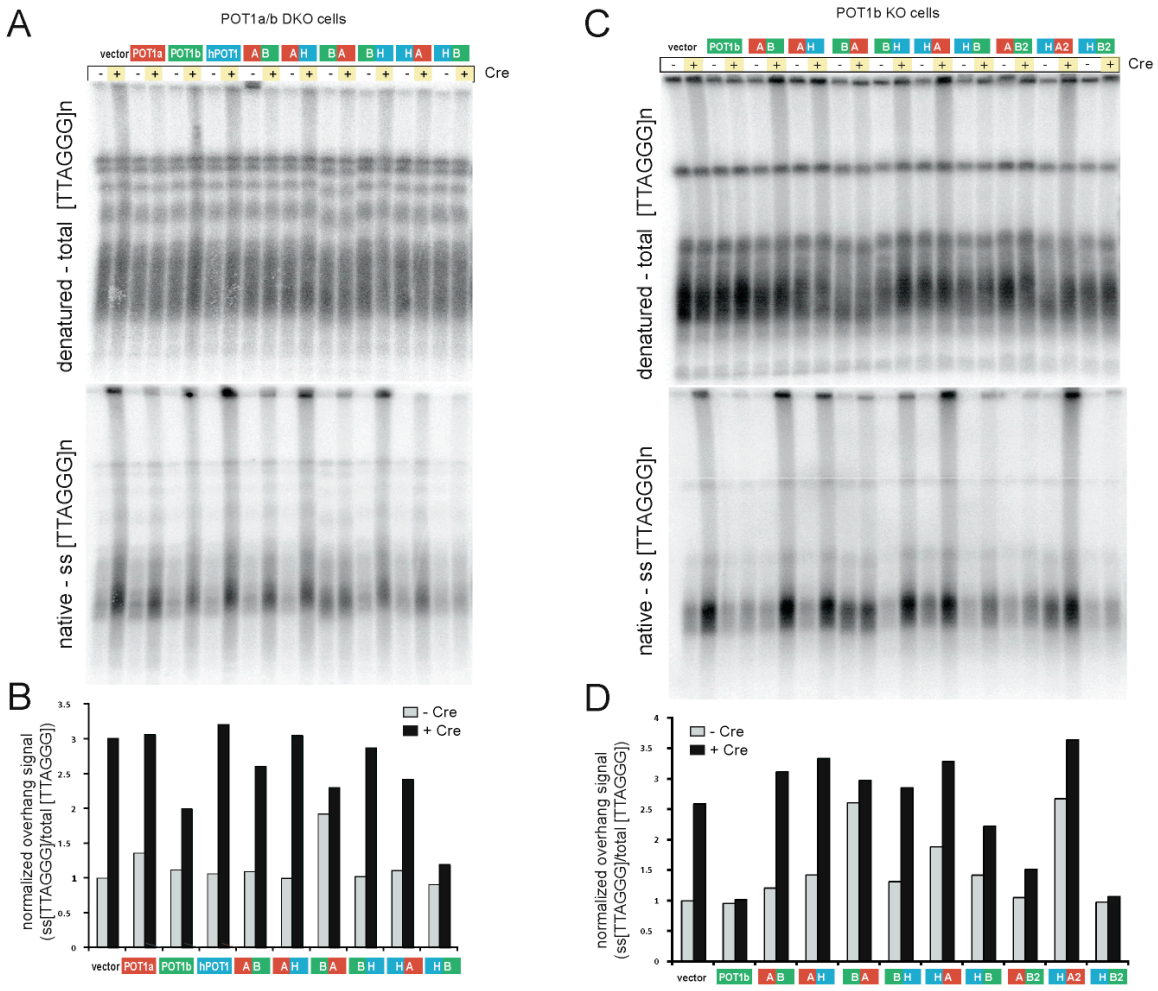

Supplemental Figure 5. Additional telomeric overhang blots of cells expressing POT1 chimeras

(A) In-gel overhang assay of MEFs conditionally targeted for POT1a and POT1b (POT1a$^{S/F}$ POT1b$^{S/F}$) expressing POT1a, POT1b, human POT1 or POT1 chimeras. Cells were retrovirally transduced with the indicated POT1 variants in pWZL-N-myc or vector control (pWZL) and selected with hygromycin. POT1a and POT1b were deleted using Hit&Run Cre and overhang length was determined 5 days after the application of Cre. (B) Quantification of the overhang signals of the cells depicted in (A). (C) In-gel overhang assay of MEFs conditionally targeted for POT1b (POT1b$^{S/F}$) expressing POT1b or POT1 chimeras. Cells were retrovirally transduced with the indicated POT1 variants in pWZL-N-myc or vector control (pWZL) and selected with hygromycin. POT1b was deleted using Hit&Run Cre and overhang length was determined 6 days after the application of Cre. (D) Quantification of the overhang signals of the cells depicted in (C). The cells described in (A) and (C) did not express human TPP1, so that POT1 variants with the human TPP1 interaction domain (human POT1, AH, BH) were not recruited to telomeres in this experiment. AB2' expressing cells represent an independent infection of POT1b$^{S/F}$ MEFs with AB2.

Supplemental Figure 6.

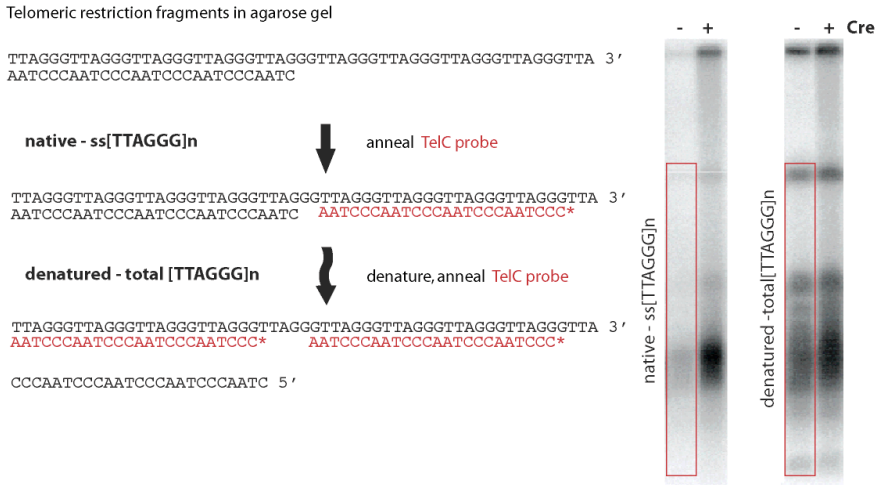

Supplemental Figure 6. In-gel overhang assay for the quantification of the telomeric 3' overhang

Schematic overview of the in-gel overhang assay. Telomeric DNA is separated by CHEF electrophoresis and hybridized with a ^{32}p-γATP end-labeled TelC probe ([CCCTAA]4). The amount of single-stranded telomeric DNA was determined by hybridization under native conditions, when only the unpaired 3' overhang is accessible to the TelC probe. Subsequently, the DNA was denatured and again hybridized with the TelC probe, yielding the amount of total telomeric DNA. Red boxes in the phosphoimager images show the regions used for the quantification of 3' overhang (native) and total telomeric DNA (denatured). Quantified overhang signals are normalized to the total telomeric signal of the same lane. In each experiment, the normalized overhang signal of the vector control – Cre was arbitrarily set to 1 and the other values given relative to this control.